Available online at www.sciencedirect.com

ScienceDirect

Energy Procedia 57 (2014) 1150 – 1159

Energy Procedia

2013 ISES Solar World Congress

Estimation of Hourly, Daily and Monthly Mean Diffuse Radiation Based on *MEO* Shadowring Correction

Alexandre Dal Pai[a], João F. Escobedo[b], Enzo Dal Pai[b], Cícero M. dos Santos[b]*

[a]*Faculdade de Tecnologia de Botucatu, Av Italo Bacchi, sn, Botucatu, 18600-000, Brazil*
[b]*Faculdade deCiências Agronômicas- UNESP – Botucatu, Brazil*

Abstract

A statistical estimate model for the anisotropic diffuse fraction as a function of clearness index K_T is proposed to estimate hourly, daily and monthly diffuse irradiations. Global, diffuse and direct solar irradiances were provided by the Laboratory of Solar Radiometry of Botucatu-UNESP (latitude 22.9º South, longitude 48.45º West, altitude 745 m). The period assigned for the study comprised the years 1996 to 2002. Global solar irradiance was measured by an Eppley PSP pyranometer, direct irradiance by an Eppley Nip pyrheliometer and diffuse irradiance by an Eppley PSP pyranometer under the Melo-Escobedo-Oliveira shadowring (radius of 40cm and width of 10cm). Isotropic and K_T corrections were applied in diffuse irradiance. The proposed model was compared to classic models reported in the literature, with good results according to the MBE and RMSE statistical indicators for hourly, daily and monthly partitions, respectively. The results showed that the inclusion of K_T correction improved the performance of the shadowring MEO according to MBE values for the three partitions: hourly, reduction from -7.21% to -1.74%; daily from -4.70% to 0.88% and monthly from -6.58% to -1.18%.

Keywords: Diffuse Radiation; Estimate Model; Anisotropy, Atmospheric Transmissivity.

1. Introduction

Information on solar potential is required in many scientific areas such as climatology, architecture, agriculture, passive lighting and satellite estimates. In general, this information is used as an input for models of energetic conversion, thermal comfort and energy balance.

Most weather stations in the world routinely measure only global solar radiation, whereas measurements of direct and diffuse radiation are less frequent due to the high cost of the devices

* Corresponding author. Tel.: 55-21-14-3814-3004;
E-mail address: adalpai@fatecbt.edu.br.

doi:10.1016/j.egypro.2014.10.102

involved. So, for locations that measure only global solar radiation, the use of statistical equations is recommended for estimation of direct and diffuse radiation [1,2].

The pioneering work for estimating diffuse radiation from global radiation was proposed by Liu and Jordan [3], correlating the diffuse fraction (ratio of diffuse to global radiation) as a function of atmospheric transmissivity (ratio of global to extraterrestrial radiation). Although this correlation was originally developed for daily values [4], several researchers have used this procedure for estimating diffuse radiation for other time-partitions, such as 5-minute average [5], hourly [6-9] and monthly partitions [10,11].

There are several estimate models in the literature relating the diffuse fraction with parameters such as altitude, latitude, solar altitude, atmospheric turbidity, water vapor, temperature, relative humidity and cloud distribution. However, the concentration of these parameters shows temporal and spatial dependence causing variability in diffuse radiation values [12,13]. In addition to these parameters, measurement techniques and instrumentation can also be sources of inaccuracy in estimate models of diffuse radiation.

1.1. MEO Shadowring Diffuse Measuring Method

Many estimate models of the diffuse fraction were developed from values of diffuse radiation measured by the shadowring measurement method because of low cost, easy maintenance and optimal operation. In this method, the ring is oriented perpendicularly to the polar axis and at an angle equal to the local latitude. It shades the band center point from sunrise to sunset. An instrument is placed at this point and allows measurement of diffuse radiation for extended periods of time. Fig 1 shows the three well-known shading setups: *Drummond*, *Robinson* and *MEO* setups.

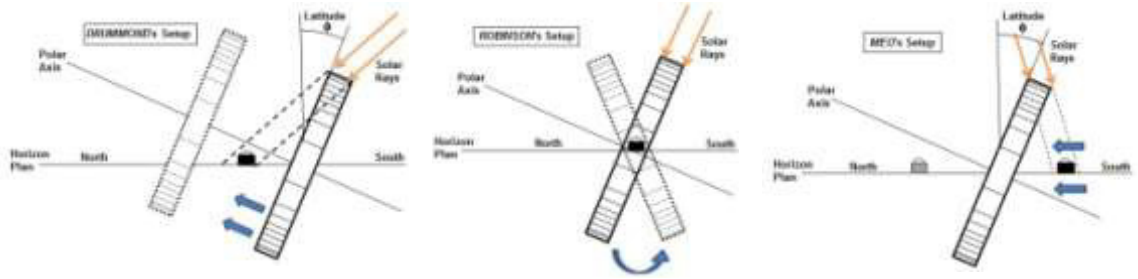

Figure 1. Shadowring setups: *Drummond*, *Robinson-Stoch* and *MEO*.

In *Drummond*'s setup, the sensor is fixed and the shadowring is translated parallelly to the polar axis to compensate the solar declination [14]; in *Robinson*'s setup, the sensor is fixed in the center of the shadowring and the shadowring is rotated around its center to compensate the solar declination [15]; in *MEO*'s setup, the shadowring is fixed and the sensor is translated parallelly to the local horizontal plan in a mobile base to compensate the solar declination [16,17].

A drawback of the shadowring method is the use of correction factors to compensate the diffuse irradiance blocked by the shadowring [14,18-21]. The correction most commonly used is based on the isotropy of the radiation, which depends on geometrical (the ring length and width) and geographical (latitude and solar declination) factors. However, the isotropic correction does not take into account the circumsolar radiation. This radiation is due to scattering of direct radiation through small angles by the atmospheric particles (aerosols, water vapor, and sky coverage) and is a result of the anisotropy of radiation.

For modeling purposes, it was expected that the best results were achieved with the diffuse radiation obtained by the difference between the global and direct radiation, since such a method does not require

correction factors. However, in this case the uncertainty is high due to the uncertainties combination of the two measuring apparatus [33]. A good alternative is the use of diffuse radiation measured by the shading disc method. Meanwhile, this method has high cost maintenance associated with solar tracking. In addition, preliminary studies for Botucatu show that the shading disc method suffers from the effects of anisotropy in the same way as the shadowring method. Thus, most estimate models use diffuse values measured by the shadowring method. However, these models underestimate diffuse radiation because only the isotropic correction is applied. Therefore, to improve the accuracy of such estimate models, a second correction based on the atmospheric transmissivity (K_T correction) is required on diffuse values [22-24].

The objective of this paper is to propose a model for estimating diffuse solar irradiation on hourly, daily and monthly mean partitions of time and compare them to classical models from the literature. The diffuse radiation was previously corrected with the isotropic and K_T corrections on 5-minute-mean time partition and the values were subsequently integrated into daily, hourly and monthly mean energetic partitions of time.

2. Methodology

2.1. Local and Climate

The present study is based upon measurements recorded by the Solar Radiometric Laboratory during the years 1996 to 2002. A total of 5 years of data were used for development of estimate models (1996-2000), while the other remaining two years were used for validation purposes (2001-2002). The Solar Radiometric Laboratory is located in the Botucatu Campus of Sao Paulo State University (22 54'S, 48 27'W, 716 m). Botucatu (Fig. 2) is a semi-rural town surrounded by sugar cane and eucalyptus crops with 127,328 inhabitants, few industries and the economy based upon services.

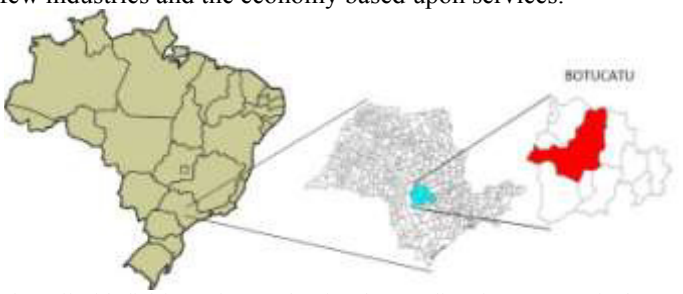

Figure 2. Map of Brazil with divisions of states showing the sampling site (Botucatu in the State of São Paulo)

According to Köppen climate classification the local climate is Cwa (humid subtropical climate - mesothermal) with hot and humid summers and dry winter. The air temperature and relative humid values follow solar astronomical variations, and maximum and minimum values are 23.12 °C (February) and 17.10 °C (July) for air temperature and 78.25% (February) and 63.97% (August) for relative humidity, respectively. The rainy season occurs in the summer and spring, with high cloudiness, when there are more than 80% of total annual rainfalls with maximum value in January (246,2 mm). In this period rainfall is convective and caused by intense evaporation of wet and heated surfaces. Rain occurs mainly in the afternoons and early evenings, it has great spatial variability, intensity is moderate to strong, and duration is short. In dry seasons (winter and autumn), monthly mean precipitation is less than 100 mm with minimum value in August (36.10 mm). In this period, rainfall is frontal caused by the meeting of cold and dry masses from the south with warm and humid masses from the Amazon region. This rain falls over a wide area, intensity is low to moderate and duration is long (hours or days) depending on the speed of the front. With regard to aerosols emitted into the atmosphere, industries and motor vehicles are the

main emitters of particulate matter. However, the study area is surrounded by 70 cities with high emissions of particulate matter as a result of burning of sugar cane, especially in the winter. The highest aerosol concentration occurs in this period due to lack of rainy days, thus preventing the deposition of particulate matter [25].

2.2. Instrumentation, Quality Control Procedure and Statistical Error Tests

Global solar irradiance I_G was measured by an Eppley - PSP pyranometer (K = 7,45 V/Wm^{-2}); direct normal solar irradiance I_b by an Eppley-NIP pyrheliometer (K = 7,59 V/Wm^{-2}) fitted to a ST-3 sun tracking device; and diffuse solar irradiance I_{dM} by an Eppley-PSP pyranometer (K = 7,47 V/Wm^{-2}) fitted to a *MEO* Shadowring (radius of 0,40m and width of 0,10m). According to [26,27], the uncertainty is 2.7% for Eppley pyrheliometer and 4.1% for Eppley pyranometers. Recent studies have shown concerns regarding the use of PSP pyranometers, limiting their application when they do not have appropriate thermal corrections [33]. The Solar Radiometric Station has additional solar radiometers used annually just for benchmarking of devices routinely used, through the comparative method.

The *MEO* Shadowring diffuse irradiance was corrected using the geometric factors proposed by [17] (eq. 1 and eq.2).

$$C_{GEOM} = \frac{1}{1 - F_{LOSS}} \tag{1}$$

$$F_{LOSS} = \left(\frac{2b}{\pi R}\right).\cos(\delta).\left[\frac{\cos(\phi+\delta)}{\cos(\phi)}\right]^2 . \int_0^{w_s} \cos(\theta_Z)dw \tag{2}$$

where b is the ring width, R the radius of the ring, δ the solar declination, ϕ the latitude, ω the hourly angle and θ_Z the zenital angle. Additional corrections were also applied and they took into account the anisotropic behavior of scattering caused by the interaction of radiation with the atmosphere. Corrections based on anisotropic parameters such as atmospheric transmissivity K_T (ratio of global to extraterrestrial radiation), zenital angle and turbidity atmospheric improve the precision of the shadowring diffuse irradiance [18] where the K_T parameter is the best representative parameter of the anisotropic conditions of the sky [22]. So, K_T corrections were proposed by Dal Pai [24] for particular K_T intervals [28] and are similar to corrections found in the literature [18-23]. The effects of optical air mass are more significant for shorter time partitions. In the present study we use longer time partitions (hourly, daily and monthly-mean), so we consider only the K_T intervals. Table 1 shows the K_T corrections for specific K_T intervals.

Table 1. Correction factors based on K_T intervals for *MEO* Shadowring diffuse irradiance.

K_T Interval	**Correction Factors**
$0 \le K_T < 0.35$	0.975
$0.35 \le K_T < 0.55$	1.034
$0.55 \le K_T < 0.65$	1.083
$0.65 \le K_T < 1$	1.108

The integrated use of geometric and K_T corrections allowed 1% difference between true and measured diffuse irradiance and shows the same order of magnitude of some correction models found in the literature [22,23,29]. The true diffuse irradiance I_{dTRUE} was calculated by the difference between global and horizontal direct irradiances given by (eq. 3).

$$I_{dTRUE} = I_G - I_B \cos\theta_Z \tag{3}$$

According to [26,27], the uncertainty of the true diffuse is 4.9% and it is a result of uncertainties of the pyranometer (global) and pyrheliometer (direct). However, true diffuse irradiance errors can reach 50–80% for clear winter skies when using a thermally-uncorrected PSP [33]. A Campbell Scientific datalogger model Cr23X was used to monitor and store solar irradiance data. The values were scanned at 5 s intervals and average values at 5 min intervals were calculated and stored. Every morning values were transmitted to a computer via a storage module model SM-192.

Solar irradiance data underwent quality control to ensure reliability of the measures. Measured values which did not fit the boundary conditions were discarded. The cut values are due to misalignment, damaged wires, lack of electricity and shadowring internal reflections due to low solar altitude. Table 2 shows the boundary conditions [29].

Table 2. Quality control filters and results.

Solar Irradiance Type	Filter
Global	$I_G < I_O$
Normal Incident Beam	$I_b \leq I_{SC}$
Shadowring Diffuse	$0.1\ I_G \leq I_{dM} < I_G$
True Diffuse	$0 \leq I_d \leq I_{SC}$

Solar irradiances were integrated into hourly and daily partitions [30]. The monthly mean partition was obtained by the daily values. Atmospheric transmissivity K_T (ratio of global to extraterrestrial irradiation) and diffuse fraction K_{DF} (ratio of diffuse to global irradiation), used for modeling purposes, were calculated by (eq. 4) and (eq. 5) for hourly, daily and monthly mean partitions and given by K_T^h, K_T^d, K_T^m and K_{DF}^h, K_{DF}^d, K_{DF}^m, respectively.

$$K_T = \frac{I_G}{I_O} \tag{4}$$

$$K_{DF} = \frac{I_d}{I_G} \tag{5}$$

The evaluation of the numerical corrections was based on mean bias error MBE, root mean square error RMSE and t test statistical indicators [31] given by the (eq. 6), (eq. 7) and (eq. 8) respectively.

$$MBE = \left(\sum_i^N (y_i - x_i) \Big/ N \right) \tag{6}$$

$$RMSE = \left(\sum_i^N (y_i - x_i)^2 \Big/ N \right)^{1/2} \tag{7}$$

$$t = \left(\frac{(N-1)MBE^2}{RMSE^2 - MBE^2} \right)^{\frac{1}{2}} \tag{8}$$

where y_i is the estimated values, x_i the measured values and N the number of observations. MBE provide information on long-term performance of a model. A positive value means an overestimation, whereas a negative one means an underestimation. A drawback of this indicator is that overestimation of an individual observation will cancel underestimation in a separate observation. RMSE provide information on the short-term performance of a model by allowing a term by term comparison of the actual difference

between the estimated value and measured value. While a high value means large scattering, a low one means little scattering. A drawback of this indicator is that a few large errors in the sum can produce a significant increase in RMSE. The Student t test allows comparison between calculated and measured values. The test also indicates whether a model is statistically significant or not in a confidence interval. The lower the t value, the better the performance of the model. T values located outside this interval (critical region) indicate that the parameter used in modeling is not statistically significant.

3. Results and Discussion

3.1. Model for estimating diffuse solar irradiation

Many models for estimating the diffuse radiation in the literature are based on the isotropy of radiation, which takes into account only the uniform spreading of the radiation striking the existing particulate matter suspended in the atmosphere. However, because of the atmospheric dynamics, this scattering is not uniform and has higher directional flow toward the earth-atmosphere. The non-uniform scattering of radiation due to different sizes of particles found in the atmosphere (aerosols and water vapor) produces the effect of anisotropy of radiation [5].

The amount of data has been reduced after the application of quality control (Tab. 3). The largest reduction occurred in hourly partition (-7.6%) because of great variability due to the optical mass near sunrise and sunset [5]. For daily and monthly-mean partitions, the reduction was 1.4% and 1.7%, respectively.

Levels of anisotropy are different for different sky coverage, increasing as the sky becomes clear [23]. In that sense, before the development of the model, the isotropic (eq. (1) and (2)) and K_T corrections (Tab. 1) were applied to the diffuse values.

The experimental values of diffuse fraction K_{DF} and atmospheric transmissivity K_T were correlated in $K_{DF}xK_T$ graphical form. Fig 3 shows the hourly ($K_{DF}^{h}xK_T^{h}$), daily ($K_{DF}^{d}xK_T^{d}$) and monthly mean ($K_{DF}^{m}xK_T^{m}$) correlations, respectively.

Some hourly and daily K_{DF} values were greater than 1 for overcast sky coverage indicating diffuse radiation higher than global radiation. This represents an improbable physical situation, since in this coverage, the direct radiation is almost zero because it is blocked by clouds, so the diffuse radiation is at most equal to the global radiation. This situation occurred because of the application of isotropic correction, especially in the summer, where this correction reaches a maximum value (25%) [17]. The region of Botucatu is characterized by two well defined seasons (dry winter with low cloudiness and humid summer with high cloudiness), with greater probability of occurrence of overcast sky in the summer, which explains an increase in diffuse radiation by up to 25% due to the application of isotropic correction. On average, this overestimation is about 2.5%, so for this reason the K_T correction factor applied is less than 1 (0.975) for this K_T interval.

Figure 3 showed that for intermediate K_T values, the scatterring of K_{DF} decreased towards increasing the partition time: greater scattering for hourly, moderate for daily and lowest for monthly-mean partitions. Shorter partitions respond faster to atmospheric dynamics, allowing a more detailed distribution of radiation and justifying the high scattering [5]. For greater partitions of time, such as daily and monthly mean partitions, the effects of atmospheric dynamics are smoothed by integrating the instantaneous values, decreasing their variability. However, specific information about the distribution of radiation is lost [32].

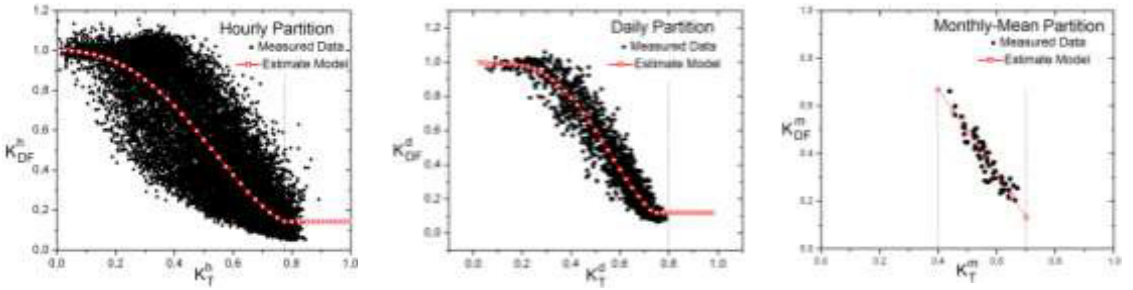

Figure 3. Diffuse fraction and atmospheric transmissivity correlations for hourly, daily and monthly mean partitions.

For clear sky coverage, K_T values greater than 0.8 indicate high atmospheric transmissivity (greater than 80%), representing an improbable physical situation (absence of atmosphere). In this case, the increase in global radiation is due to the increase in diffuse radiation caused by reflections of direct radiation in clouds on partly cloudy sky coverage, resulting in an increase in K_{DF} values, especially for shorter time partitions [5]. Therefore, values of this interval will not be considered for modeling and validation purposes.

Because of large amounts of points, it was necessary to represent K_{DF} fraction as a function of average values. The K_{DF} fraction was divided into subintervals of 0.025 of K_T for hourly and daily partitions and 0.04 for monthly mean partition. Then, the average of K_{DF} fraction for each subinterval was calculated and represented by open squares in Figure 3. Vertical dotted lines represent the limits of application of the models proposed.

Equations for estimating the hourly, daily and monthly mean diffuse fraction were proposed as a function of atmospheric transmissivity (eq. (9)).

$$K_{DF} = \sum_{n=0}^{N} A_n (K_T)^n \tag{9}$$

where A_n represents the coefficients of estimate equations, and N the degree of the polynomial. For hourly and daily partitions, a 4th degree equation was proposed, while for monthly mean a 1st degree equation was proposed, which are similar to equations found in the literature.

Table 3 shows values of hourly, daily and monthly mean coefficients for the proposed model and some coefficients for classical models of literature, with their respective intervals of validity.

Figure 4 shows the estimate models of diffuse fraction as a function of atmospheric transmissivity for hourly, daily and monthly mean partitions, respectively. Closed circles following the solid line represent the proposed model, while other lines represent estimate models from the literature. The models showed similar trends with respect to the shape of the curves, but with different quantitative levels, indicating that the estimate models show temporal and spatial dependence.

3.2. Assessment of estimate models

Estimated and measured diffuse values were compared in order to perform the validation. Measured values were obtained by the difference method (diffuse is a result of the difference between global and direct radiation). Table 4 shows results of validation of the estimate models using the MBE, RMSE and t test statistical indicators.

Table 3. Hourly, daily and monthly mean coefficients for proposed model and classical models of literature.

Models	Hourly Partition (K^h_T x K^h_{DF})					
	Interval	A^h_0	A^h_1	A^h_2	A^h_3	A^h_4
1) Proposed	0 ≤ Kt < 0.75	1.004	-0.074	-0.394	-4.886	4.733
	0.75 ≤ Kt < 1	0.143	--	--	--	--
Literature						
1) Hawlader	0 ≤ Kt < 0.225	0.915	--	--	--	--
	0.225 ≤ Kt < 0.775	1.135	-0.942	-0.388	--	--
	0.775 ≤ Kt < 1	0.215	--	--	--	--
2) De Miguel	0 ≤ Kt < 0.21	0.995	-0.081	--	--	--
	0.21 ≤ Kt < 0.76	0.724	2.738	-8.32	4.937	--
	0.76 ≤ Kt < 1	0.180	--	--	--	--
	Daily Partition (K^d_T x K^d_{DF})					
	Interval	A^d_0	A^d_1	A^d_2	A^d_3	A^d_4
1) Proposed	0 ≤ Kt < 0,73	1.005	-0.360	3.634	-14.581	10.998
	0.73 ≤ Kt < 1	0.121	--	--	--	--
Literature						
1) Newland	0.10 ≤ Kt < 0.71	0.971	0.561	-3.353	1.034	0.514
	0.71 ≤ Kt < 1	0.18	--	--	--	--
2) De Miguel	0 ≤ Kt < 0.13	0.952	--	--	--	--
	0.13 ≤ Kt < 0.80	0.868	1.335	-5.782	3.721	--
	0.80 ≤ Kt < 1	0.141	--	--	--	--
	Monthly-Mean Partition (K^m_T x K^m_{DF})					
	Interval	A^m_0	A^m_1	A^m_2	A^m_3	A^m_4
1) Proposed	0.30 ≤ Kt < 0.70	1.381	-1.783	--	--	--
Literature						
1) Lalas	0.30 ≤ Kt < 0.70	1.27	-1.45	--	--	--
2) Iqbal	0.30 ≤ Kt < 0.70	0.958	-0.982	--	--	--

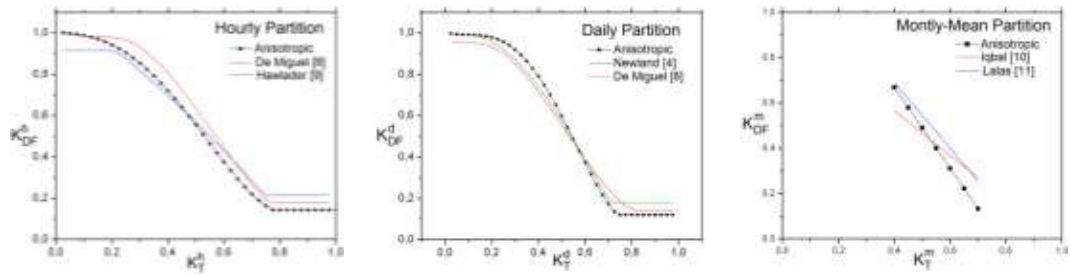

Figure 4. Diffuse fraction estimate models for hourly, daily and monthly mean partitions.

For hourly partition, although the proposed model showed the smallest value for t-test, all estimate models showed t-test values greater than the critical value, indicating that the K_T parameter used in the estimation is not statistically significant. So, more studies should be conducted in order to find out other

parameters in addition to K_T atmospheric transmissivity to explain hourly variations of the diffuse radiation. For daily partition, the proposed model was statistically significant, with t-value calculated (1.084) less than critical t-value (1.635). The other models presented t-value calculated greater than critical t-value. Therefore, they are not recommended for using in Botucatu, since they were developed for different atmospheric conditions. For monthly mean partition, the proposed model presented calculated t-value (0.665) less than the critical t-value (1.711). Therefore, this model is statistically significant to estimate the monthly mean diffuse radiation. All other models had t-values in the critical region, and therefore should not be used to estimate monthly mean diffuse radiation in Botucatu.

In general, estimate models from the literature were not suitable for estimation of diffuse radiation in Botucatu since they were designed for locations with different weather conditions and did not take into account the anisotropic aspect of radiation.

Table 4. Comparison of estimated and measured hourly, daily and monthly mean diffuse radiation for Botucatu-SP.

Models	Hourly Partition				
	N (hours)	MBE (MJ/m²)	RMSE (MJ/m²)	t_s	t_c
Proposed	7321	-0.010	0.220	3.722	1.645
Hawlader	7321	0.054	0.235	20.44	1.645
De Miguel et al	7321	0.078	0.219	32.44	1.645
	Daily Partition				
	N (days)	MBE (MJ/m²)	RMSE (MJ/m²)	t_s	t_c
Proposed	670	0.059	1.400	1.084	1.645
Newland	670	0.591	1.513	10.96	1.645
De Miguel	670	0.712	1.710	11.83	1.645
	Monthly-Mean Partition				
	N (months)	MBE (MJ/m²)	RMSE (MJ/m²)	t_s	t_c
Proposed	24	-0.079	0.571	0.665	1.711
Lalas	24	1.542	1.594	18.26	1.711
Iqbal	24	0.667	0.897	5.33	1.711

4. Conclusions

The statistical estimate model for estimating diffuse fraction as a function of atmospheric transmissivity proposed in this work showed the same tendency of polynomial models from the literature in hourly, daily and monthly mean partitions.

Results of the validation of the estimate models showed that the estimate models based on the anisotropy and isotropy of the radiation are more accurate than estimate models that take into account only the effects of the isotropy of radiation. On average, for the three partitions, the isotropic estimate model showed an inaccuracy of 6% compared to 1.5% of the estimate model that takes into account both anisotropy and isotropy effects of radiation.

Acknowledgements. The authors acknowledge the financial support from FAPESP and CNPq.

References

[1] Jain, S., Jain, P. C. 1998. A comparison of the Angstrom-type correlations and the estimation of monthly average daily global irradiation. Solar Energy, v.40, n.2, p.93-98.

[2] Jacovides, C. P., Hadjioannou, L., Pashiardis, S., Stefanou, L. 1996. On the diffuse fraction of daily and monthly global radiation for the island of Cyprus. Solar Energy, v.56, n.6, p.565-572.

[3] Liu, B. Y. H. E Jordan, R. C. 1960. The interrelationship and characteristic distribution of direct, diffuse and total solar radiation. Solar Energy, v.3, n.4, p.1-19.

[4] Newland, F. J. 1989. A study of solar radiation models for the coastal region of south China. Solar Energy, v.43, n.4, p.227-235.

[5] Suehrcke, H., Mccormick, P. G. 1988. The diffuse fraction of instantaneous solar radiation. Solar Energy, v.40, n.5, p.423-430.

[6] Skartveit, A., Olseth, J. A. 1987. A model for the diffuse fraction of hourly global radiation. Solar Energy, v.38, p.271-274.

[7] González, J., Calbó, J. 1999. Influence of the global radiation variability on the hourly diffuse fraction correlations. Solar Energy, v.65, n.2, p.119-131.

[8] De Miguel, A., Bilbao, J., Aguiar, R., Kambezidis, H., Negro, E. 2001. Diffuse solar irradiation model evaluation in north Mediterranean belt area. Solar Energy, v.70, n.2, p.143-153.

[9] Hawlader, M. N. A. 1984. Diffuse, global and extraterrestrial solar radiation for Singapore. International Journal of Ambient Energy, v.5, p.31-38.

[10] Iqbal, M. 1979. A study of Canadian diffuse and total solar radiation data - I, Monthly average daily horizontal radiation. Solar Energy, v.1, p.81-86.

[11] Lalas, D. P., Petrakis, M., Papadopoulos, C. 1987. Correlations for the estimation of the diffuse radiation component in Greece. Solar Energy, v.39, n.5, p.455-458.

[12] Zangvil, A., Aviv, O. E. 1987. On the effect of latitude and season on the relation between the diffuse fraction of solar radiation and the ratio of global to extraterrestrial radiation. Solar Energy, v.39, n.4, p.321-327.

[13] Soler, A. 1990. Dependence on latitude of the relation between the diffuse fraction of solar radiation and the ratio of global to - extraterrestrial radiation for monthly average daily values. Solar Energy, v.44, n.5, p.297-302.

[14] Drummond, A. J. 1956. On the measurements of sky radiation. Archiv. fur Meteorologie. Geophysik Bioklimatologie, v.7, pp.413-436.

[15] Robinson, H., Stoch, L., 1964. Sky radiation and measurements and corrections. Journal of Applied Meteorology, v.3, p.179-181.

[16] Melo, J. M. D., Escobedo, J. F. 1994. Medida da radiação solar difusa. In: ENERGÍAS LÍMPIAS EN PROGRESO, VII CONGRESSO IBÉRICO DE ENERGIA SOLAR, Vigo, Espanha. Anais INTERNATIONAL SOLAR ENERGY SOCIETY, v. 1.

[17] Oliveira, A. P., Escobedo, J. F., Machado, A. J. 2002. A new shadow-ring device for measuring diffuse solar radiation at surface. Journal of Atmospheric and Oceanic Technology, Boston, v. 19, p. 698-708.

[18] Kasten, F., Dehne, K., Brettschneider, W., 1983. Improvement of measurement of diffuse solar radiation. Solar radiation data, série F, n.2, p.221-225, D. Redel, Dordrecht.

[19] Dehne, K., 1984. Diffuse solar radiation measured by the shade ring method improved by a correction formula. Instruments and observing methods, Report n. 15, World Meteorological Organization, p. 263-267.

[20] Ineichen, P, Gremaud, J M, Guisan, O, Mermoud, A., 1984. Study of the corrective factor involved when measuring the difuse solar radiation by use of the ring method. Solar Energy, v.32, p 585-590.

[21] Stanhill, G., 1985. Observations of shade-ring correction factors for diffuse sky radiation measurements at the Dead Sea. Quarterly Journal of the Royal Meteorological Society, v.111, p.1125-1130.

[22] Lebaron, B. A., Michalsky, J. J., Perez, R. 1990. A simple procedure for correcting shadowband data for all sky conditions. Solar Energy, v.44, n.5, p.249-256.

[23] Battles, F. J., Olmo, F. J., Alados-Arboledas, L. 1995. On shadowband correction methods for diffuse irradiance measurements. Solar Energy, v.54, n.2, p.105-114.

[24] Dal Pai, Alexandre, Eecobedo, João Francisco, Correa, F. H. P. Numerical correction for the diffuse solar irradiance by the Melo-Escobedo shadowring measuring method In: ISES SOLAR WORLD CONGRESS 2011, 2011, Kassel.

[25] Codato, G, Oliveira, A P, Soares, J, Escobedo, J F, Gomes, E N, Dal Pai, A., 2008. Global and diffuse solar irradiances in urban and rural areas in southeast Brazil. Theor Appl Climatol, v 93, p 57-73.

[26] Reda, I.M.; Myers, D.R.; Stoffel, T.L. (2008). Uncertainty Estimate for the Outdoor Calibration of Solar Pyranometers: A Metrologist Perspective. NCSLI Measure, The Journal of Measurement Science; 3(4), pp. 58-66.

[27] International Organization of Standardization (1990), "Solar energy – Specification and classification of instruments for measuring hemispherical solar and direct solar radiation - ISO 9060:1990".

[28] ESCOBEDO, J F, GOMES, E N, OLIVEIRA, A P, SOARES, J., 2009. Modeling hourly and daily fractions of UV, PAR and NIR to global solar radiation under various sky conditions at Botucatu, Brazil. Applied Energy, v. 86, p 299-309.

[29] Kudish, A I, Evseev, E G., 2008. The assessment of four different correction models applied to the diffuse radiation measured with a shadow ring using global and normal beam radiation measurements for Beer Sheva, Israel. Solar Energy, v.82, p.144-156.

[30] Chaves M., Escobedo,J.F. A software to process daily solar radiation data.Renewable Energy, v19,n°1,p339-344,2000.

[31] Stone, R. J. 1993. Improved statistical procedure for the evaluation of solar radiation estimation models. Solar Energy, v.51, n.4, p.289-291.

[32] Suehrcke, H., Mccormick, P. G. 1989. The distribution of average instantaneous terrestrial solar radiation over the day. Solar Energy, v.42, n.4, p.303-309.

[33] Gueymard, C. A.; Myers, D.R. 2009. Evaluation of conventional and high-performance routine solar radiation measurements for improved solar resource, climatological trends, and radiative modeling. Solar Energy, v.83, p.171-185.